Contrib. Plasma Phys. **56**, No. 6-8, 754 – 759 (2016) / **DOI** 10.1002/ctpp.201610015

Effect of PFC Recycling Conditions on JET Pedestal Density*

S. Wiesen[1]**, S. Brezinsek**[1]**, D. Harting**[2]**, T. Dittmar**[1]**, E. de la Luna**[3]**, D. Matveev**[1]**, K. Schmid**[4]**,** and **JET contributors**[***]

EUROfusion Consortium, JET, Culham Science Centre, Abingdon, OX14 3DB, UK
[1] Forschungszentrum Jülich GmbH, Institut für Energie- und Klimaforschung, Plasmaphysik, 52425 Jlich, Germany
[2] CCFE, Culham Science Centre, Abingdon, OX14 3DB, UK
[3] Laboratorio Nacional de Fusin, CIEMAT, 28040, Madrid, Spain
[4] Max-Planck-Institut fr Plasmaphysik, Garching, Germany

Received 28 August 2015, revised 18 November 2015, accepted 19 November 2015
Published online 08 July 2016

Key words Edge plasma, plasma-wall interaction, pedestal, integrated modelling, ELMs.

There is experimental evidence that the pedestal dynamics in type-I ELMy H-mode discharges is significantly affected by a change in the recycling conditions at the tungsten plasma-facing components (W-PFCs) after an ELM event. The integrated code JINTRAC has been employed to assess the impact of recycling conditions during type-I ELMs in JET ITER-like wall H-mode discharges. By employing a heuristic approach, a model to mimic the physical processes leading to formation and release (i.e. outgassing) of finite near-surface fuel reservoirs in W-PFCs has been implemented into the EDGE2D-EIRENE plasma-wall interaction code being part of JINTRAC. As main result it is shown, that a delay in the density pedestal build-up after an ELM event can be provoked by reduced recycling induced by depleted W-PFC particle near-surface reservoirs. However the pedestal temperature evolution is barely affected by the change in recycling parameters suggesting that the presented model is incomplete.

1 Introduction

JET with its metallic wall consisting of a beryllium first-wall and tungsten armour in the divertor (ITER-like wall, ILW [1, 2]) has demonstrated to perform very successfully for plasma-wall interaction studies and plasma operation with the identical plasma-facing material selection foreseen in ITER [3]. It has been proven that with the ILW in JET the goal to minimize long-term fuel retention can be achieved [4, 5] and that the plasma-facing components (PFC) also do allow for a fast isotope exchange [6]. However, it has been revealed that the confinement in type-I ELMy H-mode JET discharges has degraded significantly compared to JET with a carbon wall (JET-C) at higher density. Partly, this is driven by the fact that with the ILW significant W-accumulation must be reduced to avoid a radiative collapse of the main-plasma and thus baseline ILW H-mode discharges demand higher gas-fluxes and thus recycling compared to JET-C. As a consequence in JET-ILW baseline scenarios at elevated current ($I_p > 2.5$ MA) and field a confinement factor $H98(y, 2) > 0.8$ could not be achieved so far [7]. It was also found that the confinement is impacted by the level of pumping in the divertor (which depends on divertor plasma configuration and neutral compression [8]).

Assuming stiff core plasma transport plasma the confinement is mainly driven by the pedestal performance. With the JET-ILW it was revealed that the change of the wall material has not only an impact on the pedestal parameters itself but also on the dynamics of pedestal degradation and recovery during and after an ELM [9]. For type-I ELMs in JET-C the pedestal temperature T^{ped} degradation time was similar to the MHD time $\tau^{MHD} \approx 0.2$ ms. However with the ILW for plasmas with comparable stored energies T^{ped} drops for about >1-2 ms after the ELM event, followed by a further but slower T^{ped} drop characterized by a time-scale ≈ 8-10 ms depending on

** Corresponding author. E-mail: s.wiesen@fz-juelich.de
*** See Appendix of F. Romanelli et al., 25th IAEA Fusion Energy Conference, 2014, Russia

the level of recycling. In parallel the pedestal density n^{ped} in ILW also degrades on longer time-scales compared to JET-C. The duration to reach the lowest n^{ped} after the ELM does depend on the level of n^{ped} itself. At higher n^{ped} and thus recycling the duration until full recovery of n^{ped} after the ELM increases and comes with ELM durations of a few to several ms or more. In high-recycling conditions pedestal degradation times of 8 ms or more and total recovery times >20 ms have been observed [10] leading to reduced confinement as the level of recycling increases [11]. The effect of reduced confinement is somewhat mitigated by N-seeding in discharges with high triangularity [12, 13] in which the degradation of n^{ped} can be partially mitigated.

The physical mechanism behind these observations is barely understood, if at all. State-of-the-art pedestal models like EPED1 [14] for pure deuterium fuelled plasmas with high-triangular shape predict a good agreement for the pedestal height, but the pedestal width cannot be reproduced [15]. In JET-ILW discharges with increased deuterium fueling there is no improvement in the pedestal pressure p^{ped} height but the pedestal width Δ widens that is inconsistent with the $\beta_{pol,ped}^{1/2}$ scaling expected from JET-C.

It is well appreciated that the pedestal fueling capability is directly linked with processes in the scrape-off-layer (SOL) that includes the interaction with recycling neutrals in the SOL/divertor region. We hypothesize that the change in the pedestal performance is not only connected with a change of Z_{eff} in ILW discharges (compared to JET-C Z_{eff} has decreased significantly due to the lack of C in the system) but particularly driven by the change in recycling behaviour on W/W-coated divertor plates. The experimental evidence that the recycling characteristics in the ILW is different from JET-C was discussed in [16] arguing that indeed particle recycling on W PFCs is different: the lack of co-deposited carbon layers which act as large particle reservoir is missing and high energetic particles with pedestal energies of 1keV or more can deeply penetrate (> 100 nm) into the W-PFC where particles can be confined in traps in the W solute leading to a delayed diffusive outgassing, for example, after an ELM event.

2 Integrated model description

The JINTRAC integrated code [17] is employing the 2D EDGE2D-EIRENE plasma-edge code package [18, 19] which is coupled self-consistently to the 1.5D JETTO-SANCO core plasma code [20,21]. In JINTRAC radial heat and particle fluxes (plasma and neutrals) are exchanged dynamically at a common boundary (i.e. the separatrix) and redistributed in poloidal direction [22]. The setup of the time-dependent JINTRAC integrated code model for a typical JET-ILW H-mode discharge including ELM dynamics is described in detail in [23].

The core plasma fluid transport is solved on a 1D radial grid assuming Bohm/gyro-Bohm values for particle and heat diffusion. For the inter-ELM phase within the pedestal region an edge-transport barrier (ETB) is imposed by suppressing the transport to low levels close to neo-classical values for the ions ($D^{ETB} = \chi_i^{ETB} = 0.15$ m^2/s). Electron heat transport within the ETB is assumed to be elevated by turbulent transport and imposed ($\chi_e^{ETB} = 0.15$ m^2/s). The pedestal width Δ is fixed in the model and set to ≈4 cm mapped at the outer mid-plane. The ELM model in JETTO is adhoc: an ELM is assumed to be triggered by unstable ballooning MHD modes in the edge, i.e. when the critical radial pressure gradient $\alpha_c = (2\mu_0 q^2/B^2\varepsilon)dp/d\rho$ is exceeded within the ETB. The level of α_c was acquired from the JET high-resolution Thomson scattering system (HRTS) and for the ILW type-I ELMy H-mode discharge analyzed ($I_p/B_t = 2.0$ MA/2.0 T, $P_{NBI} = 12$ MW, unseeded discharge taken from the JET-ILW C30C campaign, [4]) and $\alpha_c = 1.4$ was identified. In JETTO the ELM characteristics are set as such to expel $\Delta W_{ELM} \approx 200$ kJ of plasma energy into the SOL by increasing strongly the transport within the ETB for a short time given by the typical MHD activity time during the ELM, $\tau_{ELM} \approx 200\,\mu$s (cf. [23] for details on defining ΔW_{ELM} using the full JINTRAC model). The following levels of enhanced diffusive transport are assumed during the ELM: $D^{ELM} = 200$ m^2/s, $\chi_e^{ELM} = 100$ m^2/s, $\chi_i^{ELM} = 300$ m^2/s. After the ELM, the pedestal transport is instantaneously set back to its original ETB value allowing the pedestal to be refueled by plasma and heat transported from the core into the pedestal region by diffusion and by neutrals crossing the separatrix.

EDGE2D [18] is a 2D Braginskii edge-plasma fluid model, relaxing self-consistently in time the continuity and parallel ion momentum equations for all ionic species as well as electron and ion internal energy equations. Transport in radial direction in EDGE2D set to anomalous values. Classical Spitzer-Harm transport coefficients $\sim T^{5/2}$ are assumed for parallel electron and ion heat conductivity as well as for parallel ion viscosity and no heat-flux or viscosity limiting factors have been applied. In the JINTRAC coupling scheme, JETTO is requested

to provide EDGE2D-EIRENE new boundary conditions as input for the SOL plasma solver. The time-dependent transients of P_{SOL} and $\Gamma_\perp$ calculated by JETTO are distributed poloidally along the separatrix in EDGE2D-EIRENE. For self-consistency of the coupling the values of time varying radial transport coefficients defined by JETTO at the outer-midplane are taken as boundary values of transport in the SOL. The transport in the inter-ELM phase, i.e. the ETB values, are extended slightly into the SOL (0.5 cm at the outer mid-plane and mapped along the field lines conserving magnetic flux expansion) to allow for a realistic scaling for the heat decay parameter λ_q [24, 25] and thus $q_{||}$ along the field. Beyond λ_q in the far-SOL and throughout the divertor region the transport is increased to anomalous values of 1 m^2/s. During the ELM the transport at the separatrix is high and given by a decaying gaussian profile shape of enhanced transport in the pedestal during the ELM in JETTO [26]. A large value of the transport coefficient located at the separatrix during the ELM is reduced towards the far-SOL with exponential decay down to 1 m^2/s otherwise too large fluxes to the main-wall would occur during the ELM. Hence the dominant recycling between and at the ELM however occurs at the divertor target plates. The EIRENE Monte-Carlo neutral kinetic code is coupled to EDGE2D and providing source terms for the full set of Braginskii fluid equations. Assuming the Bohm sheath criteria as boundary condition at the target plates, plasma particles are recombining at the surface and recycled either as reflected atoms or thermally emitted molecules.

3 Revision of recycling model

In edge codes like EDGE2D-EIRENE or SOLPS the assumption of full particle recycling (recycling coefficient R = Γ_r / Γ_i = 1) is a standard assumption for steady simulations. The argument that in a carbon device co-deposited layers built up which act as infinite particle reservoirs support this assumption even for ELMy discharges. However, already a decade ago at JT-60U [27] and recently at DIII-D [28] it was suggested that the assumption of 100% recycling should be relaxed for large type-I ELMy H-mode discharges. For bulk-W or W-coated CFC divertor plates the thickness of co-deposited layers which in principle could act as particle reservoirs is small but high-energetic particles with pedestal energies can penetrate into the upper layers of the W PFCs and form near-surface reservoirs of trapped particles. The hypothesis in [16] is the following: as the W target plate is heated up during the ELM each ELM footprint acts as a mini-desorption of stored particles in the near-surface and thus depletes at least partially the reservoir of trapped D particles.

Here, in the presented rather heuristic approach a very simple near-surface reservoir model was implemented into EDGE2D-EIRENE. At each target plates a fixed number of particles can be stored in a 0D-model reservoir with particle capacity N_{cap} (i.e. the number of trapped particles which can be stored in each reservoir). At an ELM event the code checks for T_e^{plate} or T_i^{plate} at each target plate whether they exceed a given threshold ($>$ 200 eV, i.e. taking into account the time-lag of the ELM driven heat pulse as it is transported along the field until arrival at the target plate) and subsequently empties the reservoirs instantaneously. At the same time the recycling coefficient is reduced to a fixed level, namely $R^{ELM} < 1$. This will allow to pump away at least partially any particle flux arriving at a target plate after the ELM event until the reservoir is fully replenished. After filling up the reservoirs the recycling coefficient is set back to R = 1. The exact value of R^{ELM} after the ELM event is difficult to assess (cf. discussion section). Following the discussion in [3] the value of capacity N_{cap} at each target is specified as external parameter and of order $\sim 10^{20}$ D particles. The applied gas flux rate in JET H-mode discharges is typically much lower (order 10^{-2}) than the recycling flux $\Gamma_r \sim 10^{23}$ D/m^{2}s. Depending on the exact value of N_{cap} and R^{ELM} and the actual transient of the particle flux after the ELM the effective refill-time of the near-surface reservoirs at the plate can thus vary for a couple of ms as will be shown in the next section.

4 Results

JINTRAC is dynamically evolving the 1D core plasma and 2D edge/SOL plasma profiles in time and at each ELM event after exceeding the critical pedestal pressure α_c a significant fraction of the pedestal energy and particle content is flushed into the SOL. The response of the SOL is to transport the ELM driven plasma energy towards the divertor due to steepened parallel T-gradients along the field. At the same time the instantaneous increase of the upstream particle source must be equilibrated by accelerating the plasma towards the target plates. Parallel convective (free-streaming) SOL transport is fast ($\tau^{SOL} \sim L_{||}/c^s < 1$ ms) and an adaptive time-step control scheme in the EDGE2D part of JINTRAC ensures overall convergence in time. The time-scale of neutrals can be

of similar order or faster ($\tau^{neut} \sim$ 0.1-1 ms) and in the employed EIRENE model it is assumed that the neutrals can be treated in a time-independent way (in this way one has to ensure that the time between to EIRENE calls by EDGE2D is not larger than 10^{-6} s). Time-scales in the deep plasma core are much slower given by the confinement time and the inverse of the ELM frequency $1/f^{ELM}$.

By assuming an $R^{ELM} < 1$ and a finite amount of particles which can be stored for in the near-surface of the target plates, i.e. a reservoir size $N_{cap} > 0$ which is filled up by the target particle fluxes, JINTRAC can mimic the delay in particle recycling shortly after an ELM. Figure 1 a) shows for the case $N_{cap} = 10^{20}$ (at each target) and $R^{ELM} = 0.3$ the time-evolution of the particle contents N_D in each target near-surface reservoir. After the ELM, i.e. when a strong heat pulse arrives at the targets, the particles are removed from the reservoirs (i.e. pumped away). It is apparent that the model predicts a coincident arrival of the heat pulse at both targets and thus depletion of both near-surface reservoirs in the same instant. After depletion of the reservoirs and depending on the strength of the particle flux each reservoir is filled up again. Since the outer target receives a larger ion flux compared to the inner the fill-up process at the LFS target is faster.

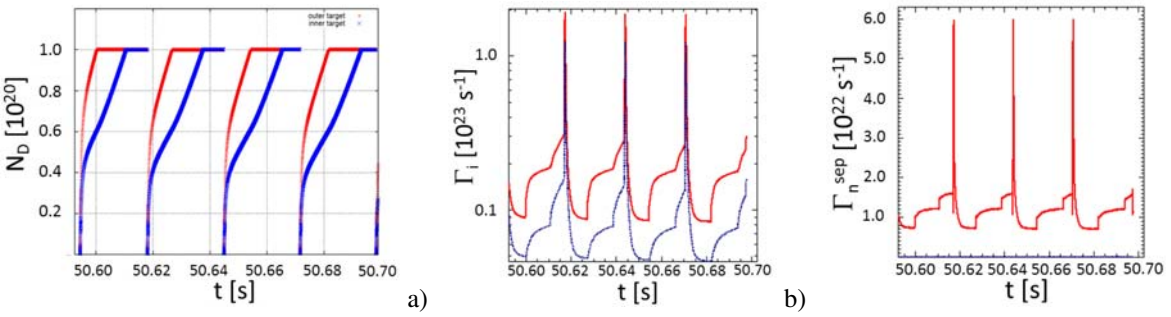

Fig. 1 For the $N_{cap} = 10^{20}$ case, with $R^{ELM} = 0.3$: a) time-evolution of the D-particle contents N_D in each target near-surface reservoir (red: outer target, blue: inner target), b) impinging ion flux Γ_i [$10^{23} s^{-1}$] at each targets, c) neutral flux Γ_n^{sep} [$10^{22} s{-}1$] crossing the sepratrix.

In Fig. 1 b) the corresponding time-evolution of the impinging ion flux Γ_i as seen by EDGE2D is shown. At ELM time the occurring peak in Γ_i is strongly reduced due to pumping of particles into the previously depleted near-surface reservoirs. After the outer near-surface is replenished, i.e. after $\sim$ 10 ms, the recycling coefficient is set back to unity only at the outer target. Then, notably at both targets, Γ_i increases steeply and saturates, until the second near-surface at the inner plate is replenished after another $\sim$ 15 ms, too. After full replenishing of both near-surface reservoirs the recycling coefficient is set back to R = 1 everywhere.

Figure 1 c) displays the evolution of the neutral flux crossing the sepratrix, Γ_n^{sep}. In the inter-ELM phase shortly after the ELM Γ_n^{sep} is decreased down to 0.8×10^{22} s^{-1}. In the approach to reach the maximum of about 1.6×10^{22} s^{-1} just before the next ELM Γ_n^{sep} increases in a step-like manner due to the imposed reduced recycling in the system. As a consequence of the delayed refuel process across the separatrix the pedestal density is retarded as seen from Fig. 2 a). We observe that n_e^{ped} is directly linked with Γ_n^{sep} as the a step-up in n_e^{ped} is synchronous with Γ_n^{sep}. From this we conclude that the pedestal refueling, although ETB transport is set back to low values shortly after the ELM (i.e. after $\tau^{MHD} = 200\,\mu s$), is driven by the neutrals entering the pedestal zone. Totally unaffected however by the change in neutral influx is the pedestal temperature, as seen in Fig. 2 b) for T_e^{ped}. It is thus concluded that heating of the pedestal for T_e^{ped} is mainly controlled by the power arriving at the pedestal top from the core and the assumed level of ETB transport.

As a result of a sensitivity scan the table 1 summarizes the derived values f^{ELM} as function of R^{ELM} and N_{cap} (assuming that all other model parameters are kept the same). We observe that by adjusting R^{ELM} and N_{cap} the amount of delay in pedestal pressure increase can be steered and thus the ELM frequency f^{ELM}. R^{ELM} is a strong parameter in the presented JINTRAC simulation and its exact value arbitrary. In table 1 also the particle fluxes across the separatrix Γ_i^{sep} and at the LFS target plate $\Gamma_i^{plate,LFS}$ are compared. Whereas Γ_i^{sep} stays nearly constant across the parameter range investigated, $\Gamma_i^{plate,LFS}$ does vary with N_{cap} and R^{ELM}. In table 1 the rightmost column identifies $F = (1 - R^{ELM})\Gamma_i^{plate,LFS}/(f^{ELM} N_{cap})$ as the ratio of an estimate of the number of particles arriving at the LFS between ELMs and reservoir size N_{cap}. The fact that F is nearly

constant suggests that in the simulations f^{ELM} is mainly driven by the target plate particle fluxes (i.e. at the LFS plate; the HFS particle fluxes are an order of magnitude lower) which in turn depend on the selection of reservoir parameters N_{cap} and R^{ELM}. After the reservoirs have filled up a finite phase with full recycling is necessary to allow for an ultimate steepening of the pedestal density gradient (the temperature gradient is nearly fixed in the simulations during the inter-ELM phase) so that the critical pressure gradient α_c can be exceeded again.

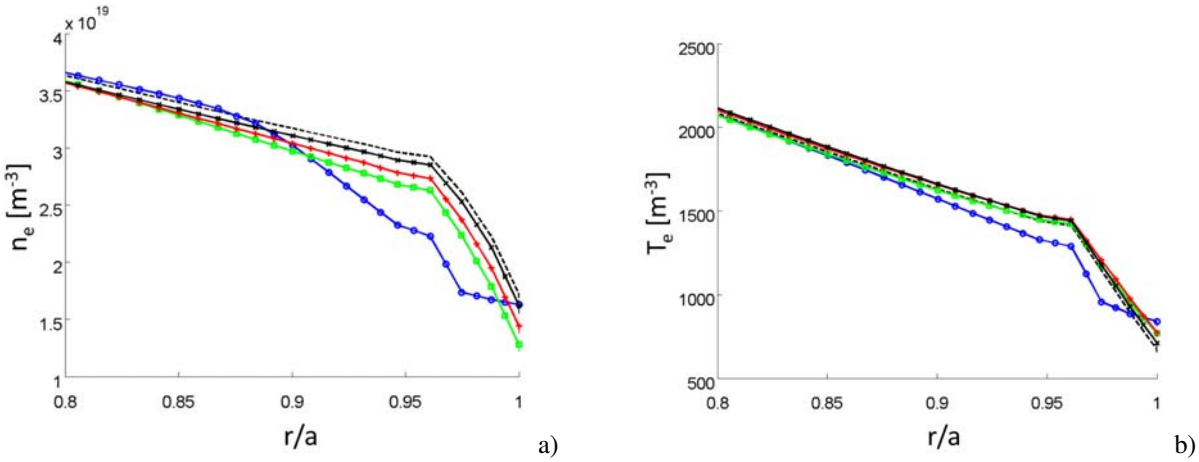

Fig. 2 Transient of the radial pedestal density profile after the modelled ELM event in JINTRAC: black/dashed: just before the ELM, blue/circles: 0.2 ms within ELM period, green/squares: 10 ms, red/pluses: 20 ms, black/crosses 27 ms. Right: Transient of the radial pedestal electron temperature.

Table 1 Sensitivity scan of R^{ELM} and N_{cap}. Γ_i^{sep} and $\Gamma_i^{plate,LFS}$ are averaged for an inter-ELM period.

R^{ELM}	N_{cap} [10^{20}]	f^{ELM} [Hz]	Γ_i^{sep} [10^{22} s^{-1}]	$\Gamma_i^{plate,LFS}$ [10^{22} s^{-1}]	F (cf. text)
1.0	-	60	0.7	7.0	-
0.5	1.0	35	1.0	2.0	2.50
0.3	1.0	33	0.8	1.2	2.40
0.5	2.0	40	0.9	4.0	2.40
0.3	2.0	20	0.8	1.3	2.28
0.2	2.0	20	0.7	1.2	2.40

5 Discussion and conclusion

By using a rather heuristic approach we have shown that a change in the recycling conditions can lead to a change in the evolution in the pedestal conditions after an ELM event. Due to unknown constraints on the used near-surface recycling parameter R^{ELM} in the sensitivity study we are currently not capable to state whether a change in the recycling conditions alone is responsible for the degrading change in confinement when moving from JET-C to the JET-ILW. Although the model does predict an impact on the post-ELM evolution of n^{ped} it does not recover the slow response of T^{ped} on the ELM as reported in [9–13]. It is very likely that other effects like a change in MHD stability after the ELM (as response to changes for example in separatrix or fueling conditions) do also play a role. However in the presented JINTRAC simulations the assumption was made that after the ELM-crash lasting for $\tau^{MHD} \sim 200\,\mu s$ the ETB transport is set back to its pre-ELM value which causes the from the experiment unexpected fast increase of T^{ped} in the post-ELM phase in the model.

A recent work by K. Schmid [29] showed that the recycling coefficient itself after the ELM is actually not changing much from unity. The model utilized in [29] is based on a 1D diffusive-trap model for the W-solute assuming isolated W traps resulting in a 0D value for a time-dependent recycling coefficient. However in [29] it was so far disregarded that a) the ELM flux footprint (target ELM wetted area) is considerably larger than

during the inter-ELM phase, and b) that the ELM driven (convective) target particle flux arrives at the same time as the heat pulse. Both assumptions are too idealistic as it has been shown by coherently averaging over many ELMs [4, 30] that the particle flux is arriving $\sim$ 1 ms later than the heat pulse, the latter significantly widening during the ELM itself. In [30] it was also reported that a pronounced secondary particle flux peak occurs 7-8 ms after the primary ELM peak.

ELM driven particles do arrive with at least pedestal energies at the target plates after the ELM event [31] and it was shown that particles with even higher energies up to 4-5 keV can exist in typical JET-ILW type-I H-mode discharges [32]. These energetic particles have the potential to penetrate deep into the material ($\gg 100$ nm from TRIM estimates) leading to supersaturation of deeper-lying layers in multi-traps [33] A delayed outgassing by diffusion out of the W-solute can be a consequence. To take this into account the heuristic model approach could be extended to allow for secondary deep-surface reservoirs allowing a refinement of the model for the outgassing process. With the JINTRAC simulations so far the strong secondary peak in the recycling flux 8 ms after the ELM could not be reproduced with the assumption of a primary reservoir only.

Acknowledgements This work has been carried out within the framework of the EUROfusion Consortium and has received funding from the Euratom research and training programme 2014-2018 under grant agreement No 633053. The views and opinions expressed herein do not necessarily reflect those of the European Commission.

References

[1] S. Brezinsek et al., J. Nucl. Mater. **415**, S936 (2011).
[2] G.F. Matthews et al., Phys. Scripta **T145**, 014001 (2011).
[3] S. Brezinsek et al., J. Nucl. Mater. **463**, 11 (2015).
[4] S. Brezinsek et al., Nucl. Fusion **53**, 083023 (2013).
[5] V. Philipps et al., J. Nucl. Mater. **438**, S1067 (2013).
[6] T. Loarer et al., J. Nucl. Mater. **463**, 1117 (2015).
[7] I. Nunes et al., IAEA-FEC, St.Petersburg, Russia (2014) EX/9-2.
[8] E. Joffrin et al., IAEA-FEC, St.Petersburg, Russia (2014) EX/P5-40.
[9] M. Beurskens et al., Nucl. Fusion **54**, 043001 (2014).
[10] E. de la Luna et al., IAEA-FEC, St. Petersburg, Russia (2014) EX/P5-29.
[11] P. Tamain et al., J. Nucl. Mater. **463**, 450 (2015).
[12] C. Giroud et al., Nucl. Fusion **53**, 113025 (2013).
[13] L. Frassinetti et al., Nucl. Fusion **55**, 023007 (2014).
[14] P.B. Snyder et al., Nucl. Fusion **51**, 103016 (2011).
[15] M. Leyland et al., Nucl. Fusion **55**, 013019 (2015)
[16] S. Brezinsek et al., to be published in Physica Scripta (2015).
[17] M. Romanelli, G. Corrigan, V. Parail, S. Wiesen, et al., Plasma Fusion Res. **9**, 3403023 (2014).
[18] R. Simonini et al., Contrib. Plasma Phys. **34**, 368 (1994).
[19] S. Wiesen et al, ITC project report (2006), http://www.eirene.de/e2deir_report_30jun06.pdf.
[20] G. Cenacchi, A. Taroni, JET-ITR(88)03 (1988).
[21] L. Lauro-Taroni et al., Proc. 21st EPS I, 102 (1994).
[22] A. Taroni et al., Proc. 16th IAEA FEC, Montreal, Canada (1996) IAEA-CN-64/D3-3.
[23] S. Wiesen et al., Plasma Phys. Control. Fusion **53**, 124039 (2011).
[24] R.J. Goldston, Nucl. Fusion **52**, 013009 (2012).
[25] T. Eich et al, Nucl. Fusion **53**, 093031 (2013).
[26] S. Wiesen et al., Contrib. Plasma Phys. **48**, 201 (2008).
[27] A.V. Chankin et al., J. Nucl. Mater. **313-316**, 828 (2003).
[28] A.Yu. Pigarov et al., J. Nucl. Mater. **463**, 705 (2015).
[29] K. Schmid et al., to be published in Physica Scripta (2015).
[30] D. Harting et al., J. Nucl. Mater. **463**, 493 (2015).
[31] W. Fundamenski et al., Plasma Phys. Control. Fusion **48**, 109 (2006).
[32] C. Guillemaut et al., submitted to Phys. Scripta (2015).
[33] D. Kato et al., IAEA-FEC St. Petersburg, Russia (2014) MPT/P7-36.

